BULLETIN OF THE POLISH ACADEMY OF SCIENCES
TECHNICAL SCIENCES, Vol. 69(2), 2021, Article number: e136723
DOI: 10.24425/bpasts.2021.136723

SPECIAL SECTION
Machine modelling and simulations

Frequency of free vibration in systems with a power-law restoring force

Ivan GREGA[1], Robert GREGA[2], and Jaroslav HOMISIN[2]

[1] Department of Engineering, University of Cambridge, Trumpington Street, Cambridge CB2 1PZ, United Kingdom
[2] Faculty of Mechanical Engineering, Technical University of Kosice, Letna 9, 042 00 Kosice, Slovakia

Abstract. To model the nonlinear behaviour of vibrating systems, Taylor expansion with integer powers is often used. Some systems, however, are inherently nonlinear. In the case of a non-integer real exponent, the power-law system cannot be linearised around the equilibrium position using Taylor expansion. The approach presented here provides a simple estimate of the principal frequency of free vibration in systems with power-law restoring force. Without seeking the precise mathematical form of the output waveform, we only focus on the principal frequency. The first step is the use of dimensional analysis to reduce the number of parameters. Two independent non-dimensional groups are formed and functional dependence between them is sought using numerical simulations. Once this dependence is known, the principal frequency of free vibration can be readily determined for any system properties and any initial conditions. Finally, we compare the numerical results to analytical expressions for a few restoring force exponents.

Key words: power-law restoring force; nonlinear vibration; dimensional analysis; numerical simulations.

1. Introduction

Vibrations are a very physical phenomenon that we experience on a daily basis. In mechanical systems, vibrations can lead to failures of machines, often giving rise to a health and safety risk to the people nearby, as well as having an adverse effect on the environment [1]. The reduction of vibration levels is therefore a very worthwhile subject. Engineering research in this area is focused on reducing vibrations below the levels imposed by regulations, which improves interactions in the man-machine-environment system [2]. Although it is presently not possible to entirely eliminate vibrations, the aim is to reduce them to an acceptable level [3, 4].

A special class of mechanical systems are those in which the primary motion is rotary. These systems give rise to torsional vibrations, which are more difficult to tackle due to other forms of energy resulting from rotary character. Rotary systems with torsional vibrations are often comprised of piston-driven machines. In spite of all the efforts to replace classical piston-driven combustion engines with their electrical counterparts, there will nevertheless remain sources of torsional harmonic excitation [5–8].

In mechanical drivetrains, the primary source of vibration is combustion engines [9]. Importantly, modern combustion engines are subject to new environmental regulations [10]. To comply with these regulations, designers often adopt approaches which, while having a positive effect on the reduction of emission levels [11], also adversely affect the content of harmonic excitation [12, 13].

Several approaches are typically used to reduce torsional vibrations in mechanical systems with piston-driven engines [14, 15]. Various types of flexible couplings and dual-mass flywheels are widely implemented [16–17]. It has been demonstrated that pneumatic tuners with adjustable torsional stiffness can be used to achieve active tuning of torsional vibrations [19–23]. Certain research ventures have focused on the application of nonlinear energy sink (NES) [24] and targeted energy transfer (TET) [25] with the goal of designing a device with quasi-zero torsional stiffness [26]. These research avenues require new approaches to solving analytical models. It is common practice in engineering that complicated systems are simplified – e.g. nonlinear systems are often linearised around an operating point. While in some cases linearisation is adequate as demonstrated in [27–29], there are applications that require nonlinear models because linearisation either does not provide sufficient accuracy, or is not possible at all [30].

The first step in extending the linear model is the addition of a cubic term. Such a system, governed by the Duffing equation, has been the subject of numerous analyses [31]. Extensive mathematical tools have been developed to model the system, whether the nonlinearity is weak or strong.

In this presented work, we decided to focus on a different type of a nonlinear system. Systems with power-law restoring force have not been extensively studied, in spite of the fact that they may occur naturally in many engineering problems. The source of nonlinearity can be contact law, such as Hertzian potential, for which restoring force f varies with displacement q as $f \propto q^{1.5}$. Further examples include systems without pre-tension or systems tuned to zero stiffness around the operating point. If the force-carrying medium is gas, such as in the pneumatic tuners [18], the restoring force is also inherently nonlinear with power-law dependence.

*e-mail: ig348@cam.ac.uk

Manuscript submitted 2020-10-30, revised 2020-12-21, initially accepted for publication 2021-01-09, published in April 2021

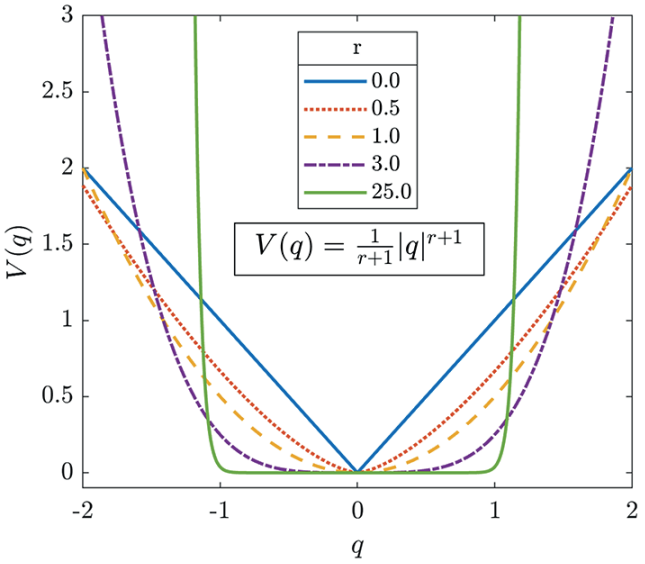

Fig. 1. Potential energy landscape for various exponents r

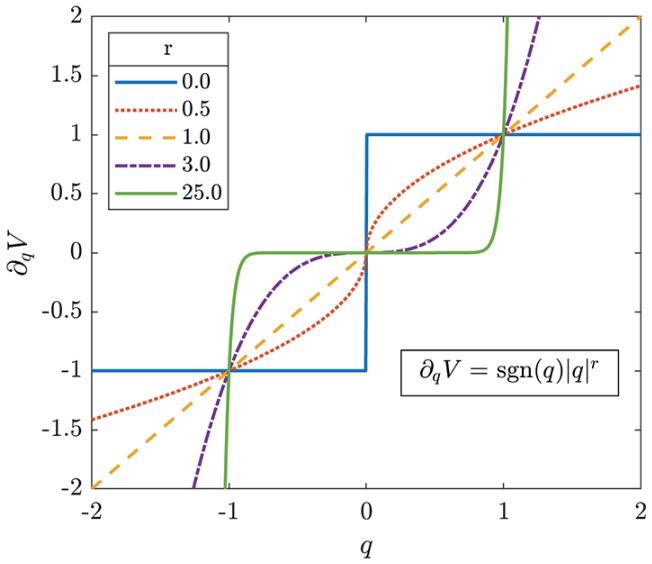

Fig. 2. Restoring force corresponding to exponents r from Fig. 1

Only relatively recently have power-law systems been described in the literature [32], where authors introduce approximate methods of solution using Jacobi elliptic functions. Our approach presented here is different. Our decision to describe the behaviour of power-law systems is partly motivated by the inherent simplicity. As will become evident, the free-vibration behaviour can be captured by two non-dimensional parameters: independent parameter r, which is the real-valued exponent in the restoring force, and dependent parameter Π_ω, which characterises the frequency of free vibration. The relationship between these two parameters is established by numerical simulations. We do not seek to mathematically describe the waveform in a general case of arbitrary exponent r. Instead, it is physically intuitive that the waveform will be periodic in nature and our only aim is to determine the principal frequency of free vibration. The structure of the paper is as follows. In Section 2 we lay down the theoretical background by describing the system that is studied and deriving the non-dimensional groups of interest. Section 3 briefly describes the methods that were used to carry out the simulations. Section 4 presents the results of the numerical simulations. In Section 5, these numerical results are compared with analytical predictions for a select few tractable cases. In Section 6 we discuss briefly the advantages and limitations of the presented work.

2. Theoretical background

2.1. Equation of motion. The potential energy in power-law system with displacement q has the general form

$$V(q) = \frac{1}{r+1}\mu|q|^{r+1}, \tag{1}$$

where $r \in \mathbb{R}^+$ and μ is a restoring force constant. This energy landscape is illustrated in Fig. 1 for various values of r.

Kinetic energy can be expressed as

$$T(\dot{q}) = \frac{1}{2}m\dot{q}^2. \tag{2}$$

Using Lagrange's equation:

$$\frac{d}{dt}\left(\frac{\partial T}{\partial \dot{q}}\right) - \frac{\partial T}{\partial q} + \frac{\partial V}{\partial q} = 0, \tag{3}$$

it follows that the equation of motion for the system in absence of damping is

$$m\ddot{q} + \mu\,\mathrm{sgn}(q)|q|^r = 0. \tag{4}$$

The restoring force $\partial_q V$ is plotted in Fig. 2 for corresponding values of exponent r. Superlinear systems $r > 1$ are *stiffening* and sublinear systems $r < 1$ are *softening*.

Equation (4) can be divided by mass m, and therefore, there remain only 2 independent system parameters: μ/m, r.

$$\ddot{q} + \frac{\mu}{m}\,\mathrm{sgn}(q)|q|^r = 0. \tag{5}$$

2.2. Dimensional analysis. Dimensional analysis, formally introduced by Buckingham [33], is a powerful tool which can be used to reduce the number of variables in a problem. Buckingham's Pi theorem states that the number of independent non-dimensional groups is given by

$$\begin{pmatrix}\text{number of}\\ \text{dimensionless}\\ \text{groups}\end{pmatrix} = \begin{pmatrix}\text{number of}\\ \text{variables}\end{pmatrix} - \begin{pmatrix}\text{number of}\\ \text{fundamental}\\ \text{dimensions}\end{pmatrix}.$$

The problem of free undamped vibration in power-law systems can be captured by the equation of motion (EOM) [5]. The system is started with initial conditions q_0, $\dot{q}_0$. The goal is to find the frequency of subsequent free vibration ω_n.

At first sight, the relevant variables in the problem are μ/m, r, q_0, $\dot{q}_0$, ω_n. There are two fundamental dimensions remaining: length L and time T. Note that the first reduction of the number of variables and number of dimensions was achieved when Eq. (4) was divided by mass m, thereby eliminating one variable and dimension of mass M. Thus, according to the Pi theorem, we should be able to form $5-2=3$ non-dimensional groups.

However, physical insight can lead to a better starting position. As presented in [34] for pure cubic system, rather than considering initial displacement q_0 and initial velocity $\dot{q}_0$ independently, they can be combined since the *total* energy in the system is important. Therefore, initial kinetic energy due to $\dot{q}_0$ can be converted into additional potential energy, yielding the *effective* initial displacement $q_{0,\mathrm{eff}}$ using the principle of energy conservation:

$$\frac{1}{2}m\dot{q}_0^2+\frac{1}{r+1}\mu|q_0|^{r+1}=\frac{1}{r+1}\mu|q_{0,\mathrm{eff}}|^{r+1}. \tag{6}$$

Therefore, both initial displacement and velocity represent the same physical quantity and for simplicity, we shall restrict ourselves to initial conditions given by

$$q(t=0)=q_0\neq 0,\quad \dot{q}(t=0)=\dot{q}_0=0.$$

Using this reasoning in dimensional analysis, the relevant variables are μ/m, r, q_0, ω_n, with two dimensions (L, T):

$$\begin{aligned}&\frac{\mu}{m}\sim L^{1-r}T^{-2}\\&q_0\sim L\\&\omega_n\sim T^{-1}\\&r\sim -\end{aligned}\quad\longrightarrow\quad \begin{aligned}&\Pi_\omega=\omega_n q_0^{\frac{1-r}{2}}\sqrt{\frac{m}{\mu}}\sim -\\&r\sim -\end{aligned}$$

Using algebraic manipulation to cancel exponents, two non-dimensional groups are obtained. According to the Pi theorem, one of the dimensionless groups is taken as dependent, and the rest are independent. The *dependent* group is Π_ω and the *independent* one is non-dimensional parameter r. Therefore, provided we included all parameters which govern the problem, the following functional dependence has to exist [33] and is sought:

$$\Pi_\omega=\Pi_\omega(r). \tag{7}$$

Another way to see the outcome of dimensional analysis is when we convert ω_n to timescale τ. Then non-dimensional group Π_ω indicates that at a given r, Π_ω is constant, and thus the timescale of vibration τ is proportional to

$$\tau\propto q_0^{\frac{1-r}{2}}\sqrt{\frac{m}{\mu}}. \tag{8}$$

As a check, the well-known formula for natural frequency of the linear system ($r=1$) is given by $\omega_n=\sqrt{k/m}$. Thus if stiffness k is replaced by μ, the period of vibration is $\tau=2\pi\sqrt{m/\mu}$, which indeed satisfies Eq. (8).

More importantly, it turns out that the linear system is the only case for which the frequency of free vibration ω_n is *independent of initial conditions* and only a function of *system parameters*. For superlinear systems, $r>1$, the exponent $(1-r)/2$ is negative, therefore, the period of vibration decreases with increasing initial displacement q_0. Such systems are also called *stiffening*. Conversely, for sublinear systems, $r<1$, the exponent is positive, resulting in *softening* behaviour, whereby the period of vibration extends with increasing initial displacement q_0.

Some useful insight has already been obtained from dimensional analysis alone. The goal of simulations is to establish the functional dependence from Eq. (7).

3. Methods

The system was simulated with initial conditions $q_0\neq 0$, $\dot{q}_0=0$ – i.e. started from rest with non-zero initial displacement.

System properties and initial conditions were chosen at random for each simulation run similarly to Monte Carlo methods in order to capture a wide spectrum of parameters and avoid the inefficacy of multidimensional grids. Let x_1, x_2 be random variables distributed according to standard normal distribution $x_1, x_2\sim\mathcal{N}(\mu=0,\sigma^2=1)$. The following were used:

$$\frac{\mu}{m}=10^{x_1}$$

$$q_0=10^{0.5x_2}.$$

MATLAB function `ode45` was used to integrate the equation of motion from specified initial conditions. In some cases, especially when power r was large ($r\sim 9$), the integration failed for some specific set of initial conditions. In this case, function `ode23` was used, which is reported to be more stable for some stiff problems.

The simulation was run for approximately 100 periods of oscillation. The non-uniform spacing of data points from MATLAB integration was linearly interpolated with number of points varying between 2^{12} and 2^{14}. The resulting waveform $q(t)$ was frequency-transformed using MATLAB's `fft` function. The frequency corresponding to the maximum amplitude in frequency spectrum was taken as the frequency of free vibration f. This was transformed into $\omega_n=2\pi f$, and using the initial condition q_0 and system properties μ/m, r, non-dimensional group Π_ω was calculated as:

$$\Pi_\omega=\omega_n q_0^{\frac{1-r}{2}}\sqrt{\frac{m}{\mu}}. \tag{9}$$

To avoid the problems with sampling and windowing, stochastic approach was used in choosing simulation time $t_{\max}$ and number of samples N_s. Let y_1, y_2 be independent random

variables distributed uniformly on the interval (0, 1) and T an estimate of period:

$$t_{\max} = (100 + 4y_1)T$$
$$N_s = \text{round}\left(2^{12+2y_2}\right).$$

4. Results of simulations

The number of simulation runs was 1000. At every run, exponent r was chosen randomly on the interval (0, 10). The remaining system parameters and initial conditions were chosen as described in the previous section.

4.1. Time and frequency data. A representative set of data obtained from one simulation is displayed in Fig. 3. Data in time domain is shown in Fig. 3a. To enable plotting of both displacement q and velocity $\dot{q}$ on the same set of axes, they were rescaled into respective non-dimensional forms $\tilde{q}, \tilde{\dot{q}}$ using appropriate length- and velocity-scales which are constant during simulation run:

$$\tilde{q} = \frac{q}{q_0}$$
$$\tilde{\dot{q}} = \dot{q}\, q_0^{-\frac{1+r}{2}} \sqrt{\frac{m}{\mu}}$$

System properties and initial conditions are shown in Fig. 3b, along with frequency-domain data.

Upon inspection of displacement and velocity-time plots, it is evident that the waveforms are *not* sinusoidal (as is the case in linear systems). The system is *stiffening* with exponent $r = 3.55$.

In the neighbourhood of equilibrium $q = 0$, both curvature $\partial_q^2 V$ and slope $\partial_q V$ of potential energy $V(q)$ are zero. Therefore, there is zero restoring force acting on the body. As a result, the slope of velocity graph $d\dot{q}/dt$ is zero when $q = 0$, which is evident in the flat top and bottom parts of velocity graph.

The frequency spectrum contains one pronounced peak at $f = 0.19$. Since displacement is not sinusoidal, higher harmonics are also present in the Fourier transform. One such component is visible in the frequency spectrum at $3f$. The fact that this frequency is three times higher than the principal frequency of vibration is not surprising, since this is the next frequency at which the cosine wave is symmetrical about the peaks of the principal-frequency wave. There are more such higher frequency components in the spectrum which are outside the x-limits of the plot.

4.2. Non-dimensional Π_ω as a function of r. Non-dimensional group Π_ω was calculated for each of the 1000 simulation runs and plotted as a function of exponent r – see Fig. 4. All data points collapse onto one curve. This confirms that dimensional analysis provided a correct non-dimensional group, since the functional dependence $\Pi_\omega = \Pi_\omega(r)$ is unique for a variety of system properties and initial conditions.

In principle, this graph provides enough information to precisely calculate the frequency of free vibration for power-law system with *any* exponent r in range(0, 10) for *arbitrary* system property μ/m and initial condition q_0. Together with the physical reasoning based on energy conservation (6), the initial conditions can be any combination of q_0 and $\dot{q}_0$.

5. Analytical modelling

It is desirable to compare the values of non-dimensional group Π_ω obtained by simulations with analytical results for certain values of r. There are three tractable cases which came to our attention: linear system $r = 1$, asymptotic limit $r \to \infty$, and limit $r \to 0$. Furthermore, an approximation using Fourier series and harmonic balance for $r \sim 1$ is calculated.

5.1. Linear system r = 1. Analysis of linear system is a classical bookwork example. The equation of motion in reduced form is

$$\ddot{q} + \frac{\mu}{m} q = 0,$$

where typically stiffness is denoted by k instead of μ.

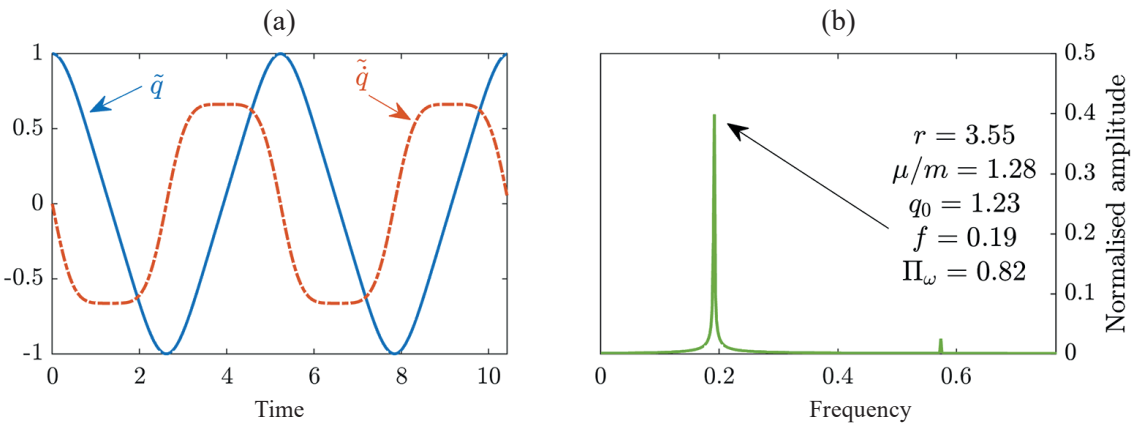

Fig. 3. Simulation results for stiffening system. a) Response in time domain: normalised velocity $\tilde{\dot{q}}$ and displacement $\tilde{q}$. b) Frequency spectrum of displacement normalised by the number of data points. The frequency of peak value taken as the principal frequency of response

System response to initial displacement $q(t=0)=q_0$ is precisely sinusoidal:

$$q(t)=q_0\cos(\omega_n t)$$

Doubly differentiating and substituting back to the EOM yields:

$$\omega_n=\sqrt{\frac{\mu}{m}}$$

This result needs to be juxtaposed with natural frequency obtained using dimensionless group Π_ω according to (9):

$$\Pi_\omega(r)=\omega_n q_0^{\frac{1-r}{2}}\sqrt{\frac{m}{\mu}} \quad\rightarrow\quad \omega_n(r=1)=\Pi_\omega(r=1)\sqrt{\frac{\mu}{m}}.$$

Therefore, we obtain:

$$\Pi_\omega(r=1)=1.$$

Examining the plot in Fig. 4, it is evident that the analytical value for Π_ω agrees very well with the value obtained from simulations.

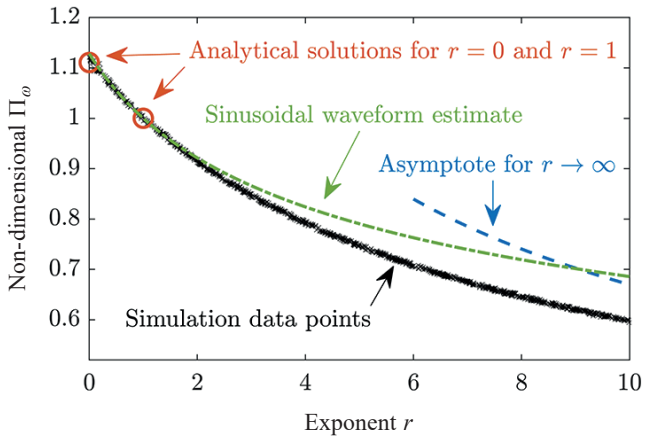

Fig. 4. Non-dimensional parameter Π_ω as a function of non-dimensional exponent r

5.2. Relay r → 0. As exponent r approaches zero, the potential energy takes up the form $V(q)=\mu|q|$. The equation of motion has the form:

$$\ddot{q}+\frac{\mu}{m}\mathrm{sgn}(q)=0.$$

The restoring force takes up one of two values: μ or $-\mu$ depending on the sign of q. A special case is $q=0$, where, for the purposes of this work, it is assumed that the restoring force is zero.

The system is often called relay, as it captures an ideal switching behaviour. Physically it could represent a system in which the magnitude of restoring force is bounded by some maximum and minimum values, and where these values are reached very shortly after departure from equilibrium. Such restoring force is hard to imagine in mechanical terms, but could well exist if it were of electromagnetic nature.

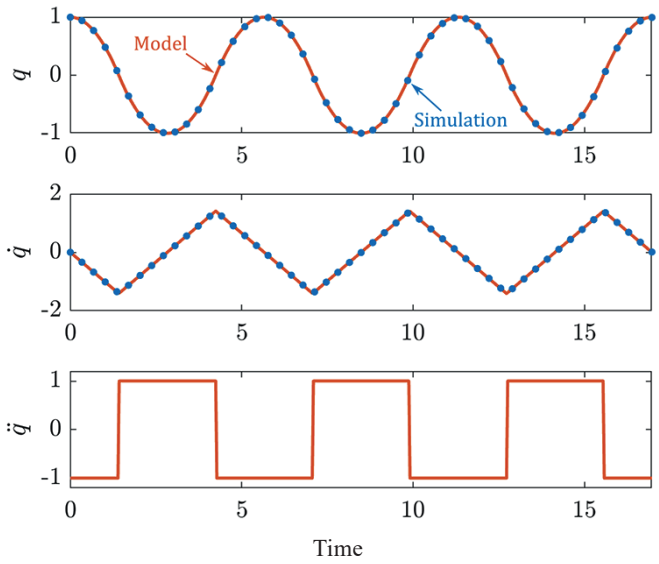

Fig. 5. System behaviour in time domain for $r\rightarrow 0$. Displacement q (parabolic piecewise), velocity $\dot{q}$ (triangular wave) and acceleration $\ddot{q}$ (square wave). Comparison of simulation data (*blue dots*, $r=0.01$) and analytical estimate according to Section 5.2 (*orange line*, $r=0$) showing an excellent match

As we assume a periodic solution, it is evident that acceleration $\ddot{q}$ will be a rectangular wave. Thus, velocity $\dot{q}=\int\ddot{q}dt$ will be a triangular wave and displacement q will be a piecewise quadratic (as shown in Fig. 5).

To obtain the time period of oscillation, we start the system with initial conditions $q(0)=q_0>0$, $\dot{q}(0)=0$. In the first instance and until displacement q becomes negative, the restoring force is $-\mu$ and acceleration is given by:

$$\ddot{q}=-\frac{\mu}{m} \quad \text{for} \quad t<t_1,$$

where t_1 is the smallest time for which $q(t_1)=0$. This equation can be integrated twice in a straightforward manner:

$$\dot{q}(t)=-\frac{\mu}{m}t,$$

$$q(t)=q_0-\frac{1}{2}\frac{\mu}{m}t^2.$$

These expressions are valid for $t<t_1$.

Thus, time t_1 is obtained by setting $q(t=t_1)=0$:

$$t_1=\sqrt{\frac{2q_0}{\mu/m}}$$

It is clear that time t_1 corresponds to one quarter of the time period. Therefore, period T and frequency ω_n are given by:

$$T=4\sqrt{\frac{2|q_0|}{\mu/m}},$$

$$\omega_n=\frac{2\pi}{T}=\frac{\pi}{2}\sqrt{\frac{\mu/m}{2|q_0|}}.$$

Similarly to the analysis for linear system, this time period needs to be compared with the result obtained using non-dimensional Π_ω. From (9):

$$\Pi_\omega(r) = \omega_n q_0^{\frac{1-r}{2}} \sqrt{\frac{m}{\mu}} \;\rightarrow\; \omega_n(r=0) = \Pi_\omega(r=0)\sqrt{\frac{\mu/m}{q_0}}.$$

Thus for $r = 0$, we obtain

$$\Pi_\omega(r=0) = \frac{\pi}{2\sqrt{2}} \approx 1.11.$$

When we compare this analytical result with simulation data in Fig. 4, there is again very good agreement.

Figure 5 shows displacement q, velocity $\dot{q}$ and acceleration $\ddot{q}$ for $\mu/m = 1$, $q_0 = 1$. There is a very good correspondence between simulation with $r = 0.01$ and analytical estimate with $r = 0$.

5.3. Oscillation between end-stops r $\rightarrow \infty$. When exponent r is large, the potential energy becomes flatter around equilibrium and grows more rapidly for larger displacements q. In the limit $r \rightarrow \infty$, the restoring force is zero except very close to the maximum displacement amplitude $q \rightarrow q_0$ and $q \rightarrow -q_0$. At maximum displacement $q = q_0$, the mass receives impulsive force and momentum is reversed almost instantly.

Such a system could be physically thought of as friction-less oscillation between hard end-stops, with perfectly elastic collisions with end-stops.

In terms of waveforms, acceleration $\ddot{q}$ will be an impulsive δ-function, velocity $\dot{q}$ will be a rectangular wave and displacement q will be a triangular wave (as illustrated in Fig. 6).

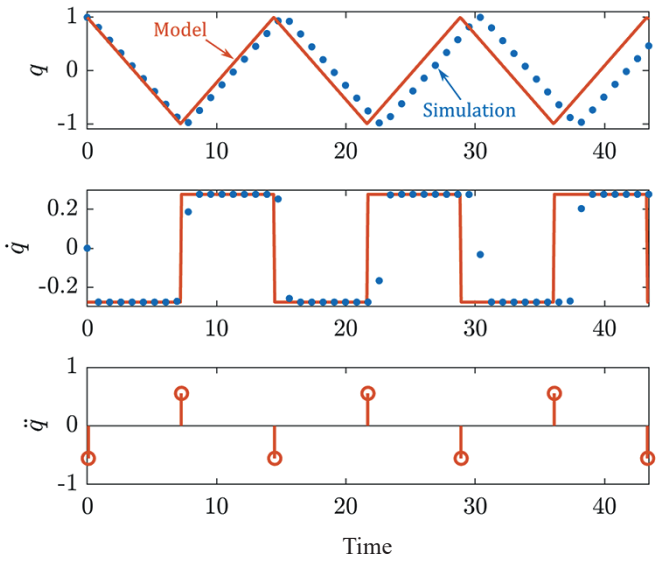

Fig. 6. Displacement q (triangular wave), velocity $\dot{q}$ (square wave) and acceleration $\ddot{q}$ (alternating impulses) for $r = 25$. Simulation data (*blue dots*) compared to triangular waveform estimate according to Section 5.3 (*orange line*) showing a 5% frequency mismatch

To calculate the period of oscillation, we first calculate the amplitude of velocity $\dot{q}_{\max}$ using conservation of energy:

$$\frac{1}{2} m \dot{q}_{\max}^2 = \frac{1}{r+1} \mu |q_0|^{r+1},$$

$$\dot{q}_{\max} = \sqrt{\frac{2\mu/m}{r+1}}\, q_0^{\frac{r+1}{2}}.$$

Let t_1 be the time when the mass reaches the other end-stop – i.e. $q(t_1) = -q_0$. Velocity and displacement for $t < t_1$ are given by:

$$\dot{q}(t) = -\dot{q}_{\max} = -\sqrt{\frac{2\mu/m}{r+1}}\, q_0^{\frac{r+1}{2}},$$

$$q(t) = q_0 - \dot{q}_{\max} t = q_0 - \sqrt{\frac{2\mu/m}{r+1}}\, q_0^{\frac{r+1}{2}} t.$$

Time t_1 is given by:

$$t_1 = 2\sqrt{\frac{r+1}{2\mu/m}}\, q_0^{\frac{1-r}{2}},$$

which is half-period of oscillation cycle ($T = 2t_1$). Therefore, frequency ω_n is:

$$\omega_n = \frac{2\pi}{T} = \frac{\pi}{t_1} = \frac{\pi}{2}\sqrt{\frac{2\mu/m}{r+1}}\, q_0^{\frac{1-r}{2}}.$$

Comparing this to the frequency obtained using non-dimensional Π_ω from (9):

$$\Pi_\omega(r) = \omega_n q_0^{\frac{1-r}{2}} \sqrt{\frac{m}{\mu}} \rightarrow \omega_n(r\rightarrow\infty) = \Pi_\omega(r\rightarrow\infty)\sqrt{\frac{\mu}{m}}\, q_0^{\frac{1-r}{2}}.$$

we obtain

$$\Pi_\omega(r\rightarrow\infty) = \frac{\pi}{2}\sqrt{\frac{2}{r+1}}. \tag{10}$$

This asymptote is plotted on Fig. 4. It can be inferred that the curve through simulation data points tends towards the asymptote as $r \rightarrow \infty$, however, for $r = 10$ there is still a significant discrepancy between the two curves.

Figure 6 shows simulation data (blue dots) for $r = 25$, $\mu/m = 1$, $q_0 = 1$. The orange lines are analytical expressions. Their frequency was obtained using the expression in Eq. (10) with $r = 25$. It is evident from the graph of displacement and velocity that this analytical estimate of frequency is not accurate. In this specific case for $r = 25$, the discrepancy is:

$$\Pi_\omega(r=25)_{\text{Simulation}} = 0.415,$$

$$\Pi_\omega(r=25)_{\text{Analytical}} = 0.436.$$

5.4. Sinusoidal waveform for $r \sim 1$. This method of estimating analytical solution for Π_ω is based on the assumption that the displacement waveform can be, to a good degree, approximated as a sine wave.

If we assume that the system response to initial displacement q_0 is sinusoidal, we have:

$$q(t) = q_0 \cos(\omega_n t),$$

$$\ddot{q}(t) = -\omega_n^2 q_0 \cos(\omega_n t).$$

Substituting back to the equation of motion, we obtain:

$$-\omega_n^2 q_0 \cos\omega_n t + \frac{\mu}{m} \operatorname{sgn}(\cos\omega_n t) |\cos\omega_n t|^r = 0.$$

To proceed further, we seek to approximate function

$$g(r, t) = \operatorname{sgn}(\cos\omega_n t) |\cos\omega_n t|^r,$$

by a cosine at the principal frequency ω_n. Therefore, term a_1 of Fourier series is sought:

$$g(r, t) = \sum_{k=1}^{\infty} a_k \cos k\omega_n t.$$

Using well-known procedures for evaluating coefficients of Fourier series

$$a_1(r) = \frac{2}{T} \int_{-\frac{T}{2}}^{\frac{T}{2}} g(r, t) \cos\omega_n t dt, \tag{11}$$

where T is given by $\omega_n = 2\pi/T$.

If $a_1(r)$ is obtained, it will be possible to proceed by balancing coefficients of cosine terms in EOM:

$$-\omega_n^2 q_0 \cos\omega_n t + \frac{\mu}{m} a_1(r) \cos\omega_n t = 0,$$

$$\omega_n = \sqrt{\frac{\mu}{m}} q_0^{\frac{r-1}{2}} \sqrt{a_1(r)},$$

and comparing the expression with the expression involving non-dimensional group Π_ω:

$$\omega_n(r) = \Pi_\omega(r) \sqrt{\frac{\mu}{m}} q_0^{\frac{r-1}{2}},$$

$$\Pi_\omega(r) = \sqrt{a_1(r)}.$$

Therefore, it remains to find coefficient a_1 according to (11):

$$a_1(r) = \frac{2}{T} \int_{-\frac{T}{2}}^{\frac{T}{2}} \operatorname{sgn}(\cos\omega_n t) |\cos\omega_n t|^r \cos\omega_n t \, dt. \tag{12}$$

Equation (12) can be reduced to

$$a_1(r) = \frac{2}{T} \int_{-\frac{T}{2}}^{\frac{T}{2}} |\cos\omega_n t|^{r+1} dt.$$

Noting that the integrand is symmetrical about $\pm T/4$, we can perform the integration on the interval where $\cos\omega_n t > 0$:

$$a_1(r) = \frac{4}{T} \int_{-\frac{T}{4}}^{\frac{T}{4}} (\cos\omega_n t)^{r+1} dt.$$

Changing variables using substitution $p = \omega_n t$ leads to Gamma function:

$$a_1(r) = \frac{2}{\pi} \int_{-\frac{\pi}{2}}^{\frac{\pi}{2}} (\cos p)^{r+1} dp = \frac{2}{\sqrt{\pi}} \frac{\Gamma\left(\frac{r+2}{2}\right)}{\Gamma\left(\frac{r+3}{2}\right)}.$$

As a check, we verify that for $r = 1$

$$a_1(r=1) = \Pi_\omega(r=1) = 1,$$

as required.

Non-dimensional Π_ω which results from this calculation is plotted as the green line in Fig. 4. It is surprisingly accurate for a range of exponents r from $r = 0$ to approximately $r = 2$. At $r = 1$, value of Π_ω is precise. For $r = 0$, we compare the value of Π_ω predicted by this sinusoidal model to the value predicted by piece-wise quadratic waveform as shown in Section 5.2:

$$\Pi_\omega(r=0)_{\text{Quadratic}} = \frac{\pi}{2\sqrt{2}} \approx 1.11,$$

$$\Pi_\omega(r=0)_{\text{Sinusoidal}} = \frac{4}{\pi} \approx 1.27.$$

The reason for such close agreement is that a piece-wise quadratic function can be very well approximated by a sinusoidal wave of fundamental period and higher-order coefficients of Fourier series a_k decay very rapidly as $1/k^3$.

For higher values of exponent r, displacement waveform $q(t)$ is becoming more triangular, and higher-order harmonics are more important. Coefficients a_k decay as $1/k^2$, thus the waveform cannot be very well approximated by the principal sinusoid. This phenomenon is observed from $r \approx 3$.

6. Discussion

One of the main differences between behaviour of power-law systems and linear systems is the dependence of frequency of free vibration. Linear systems are a special case in which the frequency of free vibrations is only a function of *system properties*. For all other power-law systems, the natural frequency of free vibrations is also a function of *initial conditions*. The non-dimensional expressions presented here provide a convenient way to calculate the natural frequency from both system properties and initial conditions. Crucially, there are only two dimensionless parameters, Π_ω and r. Taking parameter r as the independent parameter and Π_ω as the dependent parameter, a one-dimensional sweep determines the functional dependence $\Pi_\omega = \Pi_\omega(r)$. Thus, for a given power r, the value of Π_ω provides, unequivocally, the estimate of natural frequency ω_n for

any choice of system parameters m, μ and initial conditions q_0, $\dot{q}_0$. This estimate can be significant in engineering design, where an approximate estimate of the resonant frequency is sought.

The results of numerical simulations are compared with analytical expressions in select few cases. When the exact solution can be found ($r = 0$, $r = 1$), the numerical results agree precisely with the analytical values. When system response is assumed sinusoidal in vicinity of $r = 1$, the analytical estimate is based on Fourier series expansion of $\mathrm{sgn}(\cos\omega_n t)|\cos\omega_n t|^r$. This model provides relatively good accuracy until approximately $r = 2$. For higher degrees of nonlinearity, the response deviates further from sinusoidal and this estimate fails to capture the principal frequency of vibration. For high values of r, the system physically represents oscillations between end-stops and the waveform is inherently not sinusoidal. However, the convergence to the asymptotic behaviour $r \to \infty$ is quite slow. There is a middle region from $r \sim 2$ to approximately $r \sim 20$ where the natural frequency is not accurately captured by either of the two analytical models.

For such cases, we demonstrate that the reduction in number of variables by using dimensional analysis provides a convenient way to numerically determine the natural frequency for a range of initial conditions and system properties. The only assumption that is made *a priori* about the waveform of output is that it is periodic.

7. Conclusions

The focus of this article is on power-law vibrating systems which are not typically at the centre of attention in the field of mechanical vibrations. However, such a power-law restoring force can occur naturally and it is necessary to understand the behaviour of such vibrating systems. The approach to estimating the frequency of free vibration that is presented in this article is a simple method based on dimensional analysis and numerical simulations. The approach falls short of describing the shape of the waveform precisely. Instead, the main advantage of this approach is its simplicity. Instead of deriving the exact mathematical forms of oscillating quantities, only the principal frequency is sought, which can be used to guide engineering design or describe vibration phenomena.

Acknowledgements. This work was supported by the Slovak Research and Development Agency under the Contract no. APVV-19–0328 and by Lumley Curriculum Enrichment Grant of Pembroke College, Cambridge. The article was written in the framework of Grant Projects: VEGA 1/0528/20, VEGA 1/0473/17, KEGA 006TUKE – 4/2020.

References

[1] M. Moravec *et al*., "Development of psychoacoustic model based on the correlation of the subjective and objective sound quality assessment of automatic washing machines", *Appl. Acoust*. 140, 178–182 (2018).

[2] M. Puškar *et al*., "Possibilities for reducing combustion engine fuel consumption and gas emissions", *Pol. J. Environ. Stud*. 27(4), 1691–1698 (2018).

[3] L. Jakubovičová *et al*., "Impact analysis of mutual rotation of roller bearing rings on the process of contact stresses in rolling elements", *Manuf. Technol*. 13(1), 50–54 (2013).

[4] Y. Li *et al*., "Analysis on electromechanical coupling vibration characteristics of in-wheel motor in electric vehicles considering air gap eccentricity", *Bull. Pol. Acad. Sci. Tech. Sci*. 67(5), 851–862 (2019).

[5] B. Błachowski and W. Gutkowski, "Graph based discrete optimization in structural dynamics", *Bull. Pol. Acad. Sci. Tech. Sci*. 62(1), 91–102 (2014).

[6] M.P. Kazmierkowski, "Power Electronics in Renewable Energy Systems and Smart Grid: Technology and Applications", *IEEE Ind. Electron. Mag*. 13(4), 138–138 (2019).

[7] W. Jarzyna, "A survey of the synchronization process of synchronous generators and power electronic converters", *Bull. Pol. Acad. Sci. Tech. Sci*. 67(6), 1069–1083 (2019).

[8] M. Wieczorek, M. Lewandowski, and W. Jefimowski, "Cost comparison of different configurations of a hybrid energy storage system with battery-only and supercapacitor-only storage in an electric city bus", *Bull. Pol. Acad. Sci. Tech. Sci*. 67(6), 1095–1106 (2019).

[9] R. Grega *et al*., "Failure analysis of driveshaft of truck body caused by vibrations", *Eng. Fail. Anal*. 79, 208–215 (2017).

[10] THE AA: European emission standards, Limits to improve air quality and health, (2017).

[11] L. Jakubovičová *et al*., "Transport Duty Cycle Measurement of Hybrid Drive Unit for Mixing Drum", *Adv. Intell. Syst. Comput*. 393, 219–224 (2016).

[12] P. Charles *et al*., "Detecting the crankshaft torsional vibration of diesel engines for combustion related diagnosis", *J. Sound Vib*. 321, 1171–1185 (2009).

[13] M. Sága *et al*., "Modeling and experimental analysis of the aluminium alloy fatigue damage in the case of bending – torsion loading", *Procedia Eng*. 48, 599–606 (2012).

[14] L. Konieczny *et al*., "Determination of the effect of tire stiffness on wheel accelerations by the forced vibration test method", *J. Vibroengineering* 17, 4469–4477 (2005).

[15] A. Wedin, "Reduction of Vibrations in Engines using Centrifugal Pendulum Vibration Absorbers", Chalmers University of Technology, 2011.

[16] W. Sun *et al*., "Nonlinear Characteristics Study and Parameter Optimization of DMF-RS", *SAE Int. J. Passeng. Cars – Mech. Syst*. 4(2), 1050–1057 (2011).

[17] M. Zink and M. Hausner, "LuK clutch systems and torsional dampers", *Schaeffler Symposium*, 2010, pp. 8–27.

[18] R. Grega *et al*., "The Reduction Of Vibrations In A Car – The Principle Of Pneumatic Dual Mass Flywheel", *Zeszyty naukowe Politechniki Śląskiej* 84, 21–28 (2014).

[19] J. Krajňák *et al*., "The analysis of the impact of vibrations on noisiness of the mechanical system", *Pneumatyka* 17, 21–26 (2016).

[20] J. Homisin *et al*., "Removal of systematic failure of belt conveyor drive by reducing vibrations", *Eng. Fail. Anal*. 99, 192–202 (2019).

[21] J. Krajnak *et al*., "Effect of helium on mechanical properties of flexible pneumatic coupling", *Sci. J. Sil. Uni. Tech. – Ser. Trans*. 73, 63–69 (2011).

[22] P. Baran and R. Grega, "Comparison of dynamic properties of dual mass flywheel", *Diagnostyka* 16, 29–33 (2015).

[23] J. Homisin *et al*., "Continuous tuning of ship propulsion system by means of pneumatic tuner of torsional oscillation", *Int. J. Mar. Eng.: Trans. R. Inst. Nav. Arch*. 158 (A3), 231–238 (2016).
[24] Ye-Wei Zhang *et al*., "Nonlinear energy sink with inerter", *Mech. Sys. Sig. Proc*. 125, 52–64 (2019).
[25] D. Qiu *et al*., "Design of cubic stiffness for the absorber of Nonlinear Energy Sink", *CFA/VISHNO*, 2016.
[26] A. Haris *et al*., "A study on torsional vibration attenuation in automotive drivetrains using absorbers with smooth and non-smooth nonlinearities", *Appl. Math. Model* 46, 674–690 (2017).
[27] D. Maffiodo *et al*., "Finite life fatigue design of spiral springs of dual-mass flywheels: Analytical estimation and experimental results", *AIME* 10(6), 1–13 (2018).
[28] J. Homisin, "Characteristics of pneumatic tuners of torsional oscillation as a result of patent activity", *Acta Mech. Autom*. 10(4), 316–323 (2016).
[29] R. Grega and J. Krajnak, "The pneumatic dual-mass flywheel", *Sci. J. Sil. Uni. Tech. – Ser. Trans*. 76, 19–24 (2012).
[30] I. Grega and R. Grega, "Simple approach for pure cubic nonlinear vibrating systems", *Proj. bad. eks.: Tom 1. – Bielsko-Biała* 91–100 (2019).
[31] I. Kovacic and M. Brennan, "The Duffing Equation: Nonlinear Oscillators and their Behaviour", Wiley, Chichester, 2011.
[32] Z. Rakaric and I. Kovacic, "Approximations for motion of the oscillators with a non-negative real-power restoring force", *J. Sound Vib*. 330(2), 321–336 (2011).
[33] E. Buckingham, "On Physically Similar Systems; Illustrations of the Use of Dimensional Equations", *Phys. Rev*. 4(4), 345–376 (1914).
[34] I. Grega *et al*., "The potential for use of cubic nonlinear systems in internal combustion engine drivetrains", XXV Polish-Slovak Scientific Conference on Machine Modelling and Simulations, 2020.